



Contents lists available at ScienceDirect

Systematic and Applied Microbiology

journal homepage: www.elsevier.de/syapm



Diversity and bioactivities of nostocacean cyanobacteria isolated from paddy soil in Vietnam[☆]

Hang T.L. Pham^{a,b,*}, Lien T.T. Nguyen^c, Tuan A. Duong^d, Dung T.T. Bui^a, Que T. Doan^a,
Ha T.T. Nguyen^a, Sabine Mundt^e

^a Faculty of Biology, VNU University of Science, Hanoi, Vietnam

^b The Key Laboratory of Enzyme and Protein Technology, VNU University of Science, Hanoi, Vietnam

^c Institute of Biotechnology, Hue University, Thua Thien Hue, Vietnam

^d Department of Genetics, Forestry and Agricultural Biotechnology Institute, University of Pretoria, Pretoria, South Africa

^e Department of Pharmaceutical Biology, Institute of Pharmacy, Ernst-Moritz-Arndt University, 17491 Greifswald, Germany

ARTICLE INFO

Article history:

Received 25 April 2017

Received in revised form 5 August 2017

Accepted 14 August 2017

Keywords:

Cyanobacteria

Polyphasic approach

Phylogeny

Nostocaceae

Bioactivity

ABSTRACT

Nostocacean cyanobacteria are one of the important components of paddy fields due to their ability to fix atmospheric nitrogen and supply phytohormones for crop growth. In this study, 13 *Nostoc* strains isolated from paddy soils in Vietnam were classified using a polyphasic approach. The results showed a high diversity of the isolated strains that represented seven morphotypes corresponding to five genotypes, with 16S rRNA gene sequence similarity values ranging between 94.97–99.78% compared to the available sequences from GenBank. Bioassay assessment revealed that 11 out of 13 strains possessed antibacterial activities, three of which exhibited cytotoxic activities on MCF7 and HCT116 cells with an IC₅₀ ranging from 47.8 μg mL⁻¹ to 232.0 μg mL⁻¹. Interestingly, strains with identical 16S rRNA gene sequences displayed different antibacterial and cytotoxic activity profiles.

© 2017 Elsevier GmbH. All rights reserved.

Introduction

Cyanobacteria are a special photoautotrophic group of organisms that possess both atmospheric CO₂ and N₂ fixation capacity. Independently of organic carbon and nitrogen sources, they can occur in all types of habitats, even in extreme environments such as hot springs, deserts, and in the Antarctic. The incredible variety of niches inhabited by cyanobacteria are attributed to their diversity and ability to produce a large number of defensive metabolites [41,42]. To date, a huge number of bioactive compounds, including phenolics, alkaloids, terpenoids, steroids, polyketides, peptides, phytohormones and halogenated compounds, have been discovered from cyanobacteria [32,44]. Thus, cyanobacteria have been considered as a potential source for drug development [8,12]. So far, most of the isolated compounds were derived from cyanobacterial strains in Europe and America, as opposed to those from Asia,

have been suggested as promising sources for finding new entities [49].

In Vietnam, cyanobacteria are frequently found in lakes, ponds and, especially, rice fields. They have mainly been utilized as biofertilizers for rice and crops due to their nitrogen fixing ability rather than as producers of bioactive compounds. However, recently, some novel compounds, such as carbamidocyclophanes A–E [6] and nhatrangins A–B [9], have been discovered from Vietnamese cyanobacteria. In another study, following investigation of 14 cyanobacterial strains from Vietnam, it was found that *Nostoc* sp. CAVN2 could produce over 60 cyclophane-like compounds. Among these, five compounds were new carbamidocyclophanes that exhibited potent antimicrobial activity against methicillin-resistant *Staphylococcus aureus* [36]. These studies have demonstrated that cyanobacteria from Vietnam could represent a potential source of novel bioactive compounds with pharmaceutical importance.

The *Nostocaceae* represent a large family consisting of unbranched filamentous cyanobacteria (isopolar or heteropolar) with special prominent cells (heterocytes, akinetes). This family is a challenging group for classifying into monophyletic genera, and thus many genera have been arguably designated as polyphyletic [27,41]. In the past, taxonomic classification of cyanobacteria was based solely on morphological characteristics, which has

[☆] Partial 16S RNA gene sequences are available in GenBank under accession numbers KY818310–KY818314.

* Corresponding author at: VNU University of Science, 334 Nguyen Trai, Thanh Xuan, Hanoi, Vietnam.

E-mail addresses: luonghang@hus.edu.vn, pham.hang@uni-greifswald.de (H.T.L. Pham).

been considered inefficient for modern taxonomy because many morphology characters could be altered under different growth conditions [28]. Moreover, a number of taxa have been delimited based on slight morphological differences (e.g. sheath characteristics, a slight derivation in cell dimensions or filaments) that did not always coincide with the variability of 16S rRNA gene sequences [24,41]. To address these limitations, Hoffmann et al. [18] proposed the polyphasic approach in which genetic characterization would become a primary criterion in combination with morphological and ecological analyses. Based on this approach, evolutionary relatedness has led to the successful classification of many nostocacean strains from diverse habitats, such as freshwater bodies in Belgium and Luxembourg [54], thermal springs in Greece [5] and mangroves in Brazil [43]. This approach has also been used to redefine the traditional genus *Nostoc* into the core *Nostoc* clade (*Nostoc sensu stricto*) and to introduce new genera to accommodate phylogenetically coherent lineages [16,20,27].

To date, the polyphasic approach has been considered to be a unique and fully acceptable methodological procedure for obtaining a correct taxonomic classification of cyanobacteria [25]. Despite the numerous studies on either the molecular phylogeny [7,14,22,24,31,34,37] or bioactivities [13,19,21] of nostocacean cyanobacteria, the relationship between phylogenetic relatedness and the ability to produce bioactive compounds among the strains has not been sufficiently addressed. Therefore, in this study, the diversity of cyanobacteria isolated from paddy fields in Vietnam was studied using 16S rRNA gene sequences, and their ability to produce bioactive compounds was investigated and compared.

Materials and methods

Sampling sites

Paddy soil samples were collected from the Phu An, Phu Duong, Phu Ho, and Phu My communes in Phu Vang district, Thua Thien Hue province, Vietnam (between 16°37'–16°55'N latitude and 107°56'–107°72'E longitude) from February 2012 to November 2013. Soil samples were taken from three different positions at each study site.

Cyanobacteria isolation

In the laboratory, each soil sample was suspended in liquid BG11 medium [39], and 5 mL of the suspension was subsequently applied to a sterilized filter paper placed in a Petri dish. All Petri dishes were incubated under white fluorescent irradiation ($10 \mu\text{mol m}^{-2} \text{s}^{-1}$) for 2 weeks in order to obtain growth of cyanobacteria. Single colonies of cyanobacterial strains were isolated using an agar plate spreading technique [2]. Axenic strains were obtained by treatment of the culture with $10 \mu\text{g mL}^{-1}$ augmentin (four parts amoxicillin trihydrate: one part potassium clavulanate; Sigma–Aldrich, USA). After antibiotic treatment, either cyanobacterial cells or culture media were spread onto Luria–Bertani agar medium (Sigma–Aldrich, USA) to confirm the absence of heterotrophic bacteria. All axenic strains were deposited in the cyanobacteria culture collections of the Faculty of Biology, VNU University of Science, Hanoi and the Institute of Biotechnology, Hue University, Vietnam.

Morphological characterization

Morphological examination was carried out using Olympus CK40 and Nikon Eclipse 551 microscopes equipped with digital cameras. Photographs were taken from cultures in the exponential phase of cyanobacterial growth.

The cell dimensions (length and width of vegetative cells, heterocytes and akinetes) of different filaments of each axenic

strain were measured from both live and preserved materials, and, where relevant, at least thirty morphometric measurements were made per structure (cell and filament) and the averages were calculated. Species identification was carried out following the classification system of Komárek et al. [27]. Taxonomic identification was based on characteristic morphological keys from the traditional cyanobacterial taxonomy literature, such as Geitler [15], Desikachary [11], Komárek and Anagnostidis [26].

DNA extraction

Cyanobacterial cultures were grown in BG11 medium for one week. Biomass was harvested and DNA was extracted using the PrepMan® Ultra Sample Preparation Reagent (Applied Biosystems, USA). Approximately 50 mg of fresh biomass were added to a 1.5 mL micro-centrifuge tube, to which 100 μL of PrepMan reagent were added. The tube was incubated for 5 min at 96 °C. The biomass was homogenized inside the tube using a micro-pestle. The tube was incubated for another 5 min at 96 °C, and thereafter centrifuged at $12,000 \times g$ for 10 min. The supernatant was transferred to a new tube diluted five times with 10 mM tris–HCl pH 8.0. This crude-extract DNA solution was kept at –20 °C and was used directly as template in PCR reactions.

PCR amplification and sequencing of 16S ribosomal RNA

Part of the 16S rRNA gene region was amplified using primer 1 (5'-CTC TGT GTG CCT AGG TAT CC-3') and primer 2 (5'-GGG GGA TTT TCC GCA ATG GG-3') [3] that can also amplify the entire ITS region, although the ITS sequences were not considered in this study. The PCR reaction mixture consisted of 2.5 μL 10 \times PCR reaction buffer, 2.5 mM MgCl_2 , 200 mM of each dNTP, 0.2 mM of each forward and reverse primers, 1 U FastStart Taq DNA Polymerase (Roche Applied Science, Germany), 2 μL extracted DNA solution, and PCR grade water to a final volume of 25 μL . The PCR thermal cycle consisted of an initial denaturation step at 96 °C for 5 min, followed by 35 cycles of 95 °C for 30 s, 55 °C for 20 s, 72 °C for 1 min, and a final extension at 72 °C for 10 min. After PCR amplification, one unit of exonuclease and one unit of thermosensitive alkaline phosphatase (Thermo Fisher Scientific, USA) were added to each of the PCR products, and the tube was then heated at 37 °C for 15 min followed by 80 °C for 15 min. The enzyme-treated PCR products were sequenced with primer 1 [3] and primer 6 (5'-GAC GGG CCG GTG TGT ACA-3') [4], which only targeted the 16S region, rather than the ITS region, of the PCR amplicons obtained. The sequencing reactions were carried out using the BigDye™ Terminator 3.1 cycle sequencing premix kit (Applied Biosystems, USA) following the manufacturer's protocols.

Phylogenetic analyses

Consensus sequences were assembled from forward and reverse sequencing reads using the CLC Genomics Workbench v8.0.1 (CLCBio, Denmark). BLAST searches were conducted with all sequences obtained from this study against the GenBank nucleotide database, from which most closely related sequences were downloaded and included in the subsequent phylogenetic analyses. Additional sequences representing genera closely related to *Nostoc*, namely *Desmonostoc*, *Halotia*, *Mojavia* and other related taxa, were also downloaded and included in the analyses. A preliminary analysis was conducted and the result was used to refine the dataset further. Only the sequences most related to those obtained from this study and sequences representing relevant lineages were included in the final analysis. The dataset was aligned using MAFFT v7.221 [23], trimmed at both ends, and thereafter subjected to maximum likelihood (ML) and Bayesian inference (BI) analyses. jModelTest v2.1 [35] was used to determine the best fit substitu-

tion model. ML analysis was performed with RaxML v8.2.9 [46], and ten runs with a GTR+G+I model and 1000 bootstrap replications were conducted. BI analysis was performed with MrBayes v3.2.5 [40], and ten MCMC runs were conducted using a GTR+G+I substitution model. Trees were sampled every 100th generation and runs were set to stop when the average standard deviation of split frequencies reached 0.01 or lower, and burn-in was set to a 0.25 fraction of the trees sampled.

Batch cultivation and harvesting

Each axenic strain was cultivated in 500-mL Erlenmeyer flasks containing 300 mL sterile BG11 medium inoculated with 5 mL of a three-week-old stock culture of the strain. All strains were grown at 24 °C under a 12:12 light/dark cycle with white fluorescent irradiation ($30 \mu\text{mol m}^{-2} \text{s}^{-1}$). The cyanobacterial biomass was harvested after 7–8 weeks by centrifugation at $6000 \times g$ for 10 min at 20 °C, followed by lyophilization, and storage at –20 °C. For comparison of bioactivities, all 13 strains were cultivated under identical nutrient, temperature, and light/dark cycle conditions.

Preparation of extracts

For bioactivity screening, freeze-dried cyanobacterial cells were successively extracted with two organic solvents following the procedure described in a previous study with minor modifications [36]. Firstly, 2 g dried biomass from each strain was homogenized in 100 mL ethyl acetate using a mortar and pestle, followed by sonication for 5 min and stirring for 60 min at room temperature. The homogenized solution was centrifuged at $5000 \times g$ for 10 min at 20 °C and the supernatant was collected by filtration. The residue was extracted once again with 100 mL ethyl acetate and all supernatants were combined to obtain an ethyl acetate extract. Dried residue was then successively extracted twice with 100 mL methanol, according to the same procedure, in order to obtain the methanol extract. The organic solvents were removed by vacuum rotary evaporation. The dried extracts were weighed and stored at –20 °C until use.

Cytotoxicity assays

The Sulforhodamine B (Sigma–Aldrich, USA) kit was used for evaluation of cytotoxic activity of cyanobacterial extracts. Three cancer cell lines were used for this test, including breast adenocarcinoma cells (MCF7 ATCC HTB-22), colon carcinoma cells (HCT 116 ATCC CCL-247), and hepatocellular carcinoma cells (HepG2 ATCC HB-8065). Cells were seeded in a 96-well microplate, with 5000 cells/well in 180 μL culture medium (DMEM/RPMI 1640; Sigma–Aldrich, USA) and cultivated at 37 °C in 5% CO_2 /95% air for 24 h. After the incubation period, each well was supplemented with 20 μL cyanobacterial extracts at a final concentration of 400, 200, 100, 50, or 25 $\mu\text{g mL}^{-1}$. Each concentration was tested in four parallel replicates and the experiment was repeated three times. Paclitaxel (Sigma–Aldrich, USA) was used as a positive control at concentrations ranging from 0.003 $\mu\text{g mL}^{-1}$ to 30 $\mu\text{g mL}^{-1}$. After 48 h, cells were dyed with sulforhodamine B and the optical density of the cells was measured using a Microplate Reader Model 680 (Bio–Rad, USA) at a wavelength of 540 nm [52]. The IC_{50} values (the concentration of extract at which 50% of cell growth was inhibited) were calculated by Excel and GraphPad Prism 6.1 software.

Agar diffusion assay

Four bacterial strains, including both Gram-positive bacteria (*Staphylococcus aureus* ATCC 25923 and *Bacillus subtilis* ATCC 6633) and Gram-negative bacteria (*Salmonella typhi* ATCC 14028 and

Shigella flexneri ATCC 12022), were used as test organisms. All crude extracts were prepared at a concentration of 40 mg mL^{-1} methanol and an aliquot of 50 μL was loaded onto paper discs (Whatman \varnothing 6 mm). Methanol (50 μL /paper disc) was used as a negative control. After evaporation of methanol, the paper discs were applied to an agar plate containing test bacteria and kept at 4 °C for 3 h. The agar plate was then incubated at 37 °C for 24 h. The diameters of the inhibition zones were measured over the whole zone including the paper disc [6].

Results

Morphological characterization

The 13 isolated strains were divided into seven morphotypes based on their shape, as well as the dimensions of the filaments, vegetative cells, heterocytes and akinetes. Of the 13 strains, seven strains, including APA4, APA5, APA9, NPA1, NPA6, APD3 and APD4 (Figs. 1–3), were grouped into a single morphotypic group (indicated as morphotype I) and their morphological characters resembled the description of *Nostoc calcicola* Breibisson ex Bornet & Flahault [11,26]. Their trichomes were straight or slightly curved, densely aggregated in a gelatinous layer, and the terminal cells were usually cylindrical or rounded conical. The heterocytes were located terminally or intercalary, and the akinetes frequently occurred in series. However, the parameters of vegetative cells, heterocytes, and akinetes were slightly variable (Table 1). Strains formed dark-blue filaments, except those of APA4 and APD3 that were light blue–green and a dull olive color, respectively.

The six remaining cyanobacterial strains were different from each other by one or more characteristics corresponding to six single morphotypes. The morphological characteristics of strain APH5 were similar to those of morphotype I, despite the fact that its trichomes were arranged in parallel as a blue mucous cluster (Fig. 4, 36–38) [11]. Strain NPA12 formed tetraspores during sporulation, similar to APA5, but the size of the vegetative cells was 1.5–2.0 times larger (Fig. 5, 47–52). Strain APH4 had a more or less smaller trichome diameter (2–2.5 μm) with an olive color (Fig. 5, 57–59). While APM3 had straight trichomes arranged in parallel, its colonies were flag-shaped, 3–4 mm thick, and embedded in yellowish green to yellowish brown colored mucilage (Fig. 5, 53–56). Strain PA2 possessed a distinct sheath layer and large akinetes in series of 5–10 (Fig. 4, 42–46). Strain NMA2 showed a clearly distinct morphology, since it was a light blue–green color with square, short vegetative cells, oblong heterocytes, and conical- or arrow-shaped terminal cells. Its vegetative cells, heterocytes, and akinetes were the smallest in comparison to all the other strains (Fig. 4, 39–41). However, the observed morphology and morphometry of all six morphotypes did not provide strong enough support to classify them into any of the designated morphospecies.

Molecular phylogeny and sequence comparison

The compiled dataset of 16S rRNA gene regions included 76 taxa. This dataset consisted of 919 characters including alignment gaps, of which 298 were variable and 196 were informative characters. MrBayes runs reached desired coverage after 1,580,000 generations where the average standard deviation of split frequencies was 0.009954. Phylogenetic trees obtained from ML and BI analyses had similar topologies. However, the Bayesian tree analysis had much better support for many of the nodes not supported by ML analysis. All 13 strains identified in this study corresponded to five genotypes, and these, together with other reference *Nostoc* spp. from the GenBank database, were divided into two major phylogenetic clades (clade A and clade B) (Fig. 6). The phylogram obtained from

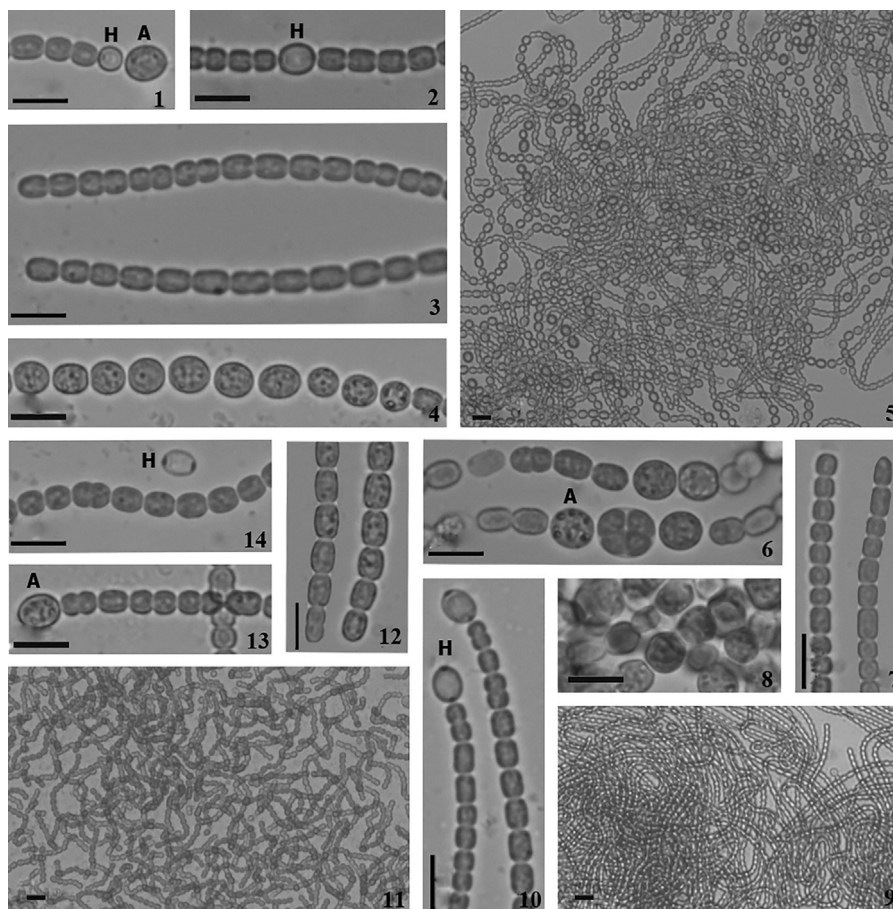


Fig. 1. 1–5. Strain APA4. 1 – Trichome with heterocyte (H) next to akinete (A). 2 – Trichome with cylindrical heterocyte. 3 – Cylindrical vegetative cells in straight trichomes. 4 – Akinetes in series in old culture. 5 – Trichomes in a mass. 6–10. Strain APA5. 6, 8 – Trichomes with akinetes. 7 – Vegetative filaments. 9 – Trichomes in a mass. 10 – Trichomes with heterocytes. 11–14. Strain APA9. 11 – Trichomes in culture. 12 – Straight trichomes. 13 – Oval akinete. 14 – Heterocyte. Scale bars = 10 μm. A: Akinete; H: Heterocyte.

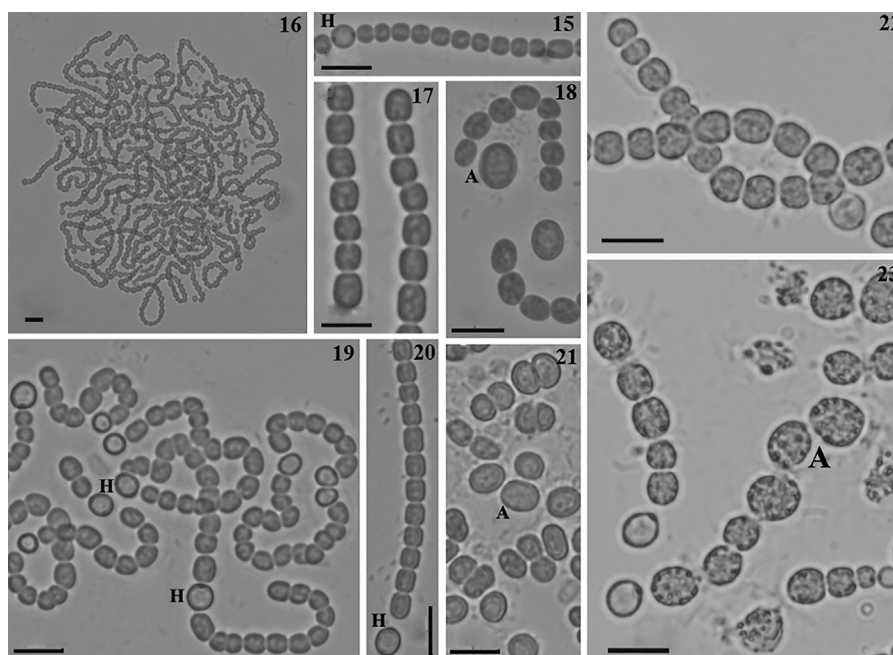


Fig. 2. 15–21. Strain NPA6. 15 – Trichome with heterocyte (H). 16 – Trichomes in a mass. 17– Straight trichomes. 18–21 Trichomes with heterocytes (H) and akinetes (A). 22–23. Strain NPA1. 22 – Vegetative trichomes. 23 – Akinetes in series. Scale bars = 10 μm.

Table 1
Morphological characters and geographical origin of 13 cyanobacterial strains used in this study.

Strains	Thallus color	Trichome features	Vegetative cell (μm)		Heterocyte (μm)		Akinete (μm)		Terminal cell (μm)	Geographical origin
			Width	Length	Width	Length	Width	Length		
APA4	Light blue–green	Straight or slightly curved, densely aggregated in gelatinous layer	2.5–5.0	3.0–8.0	6.0–7.0	8.0–9.0	8.0–10.0	9.0–12.0	Cylindrical or rounded conical	Phu An
APA5	Dark blue–green	Straight or slightly curved, densely aggregated in gelatinous layer	2.5–3.0	3.5–4.5	6.0–7.0	7.0–8.0	5.6–6.0	6.0–9.0	Cylindrical or rounded conical	Phu An
APA9	Dark blue–green	Straight or slightly curved, densely aggregated in gelatinous layer	2.5–3.3	2.5–5.0	3.0–6.0	3.0–6.0	6.0–6.5	6.5–7.0	Cylindrical or rounded conical	Phu An
NPA1	Dark blue–green	Straight or slightly curved, densely aggregated in gelatinous layer	5.0–6.0	5.0–10.0	4.0–6.0	6.0–8.0	7.0–10.0	8.0–14.0	Rounded or rounded conical	Phu An
NPA6	Dark blue–green	Straight or slightly curved, densely aggregated in gelatinous layer	2.5–3.0	5.0–7.0	4.0–7.0	4.0–7.0	5.0–7.0	7.0–10.0	Cylindrical or rounded conical	Phu An
APD3	Olive–green	Straight or slightly curved, densely aggregated in gelatinous layer	3.0–3.5	5.0–6.0	4.0–5.0	5.0–6.0	5.0–10.0	7.0–12.0	Rounded conical	Phu Duong
APD4	Dark blue–green	Straight or slightly curved, densely aggregated in gelatinous layer	2.5–3.0	3.0–4.0	3.5–4.0	4.0–5.0	5.0–8.0	5.0–9.0	Cylindrical or rounded conical	Phu Duong
APH5	Pale blue	Arranged parallel in a blue mucous cluster	3.5–4.0	4.0–5.0	6.0–7.0	6.0–7.0	9.0–10.0	12.0–14.0	Rounded conical	Phu Ho
NMA2	Light blue–green	Straight or slightly curved in mucus	2.5–3.0	2.5–3.0	3.0–4.0	4.0–7.0	5.0–6.0	6.0–7.0	Conical or arrow	Phu Duong
APH4	Olive color	Straight or slightly curved, in mucus	2.0–2.5	4.0–5.5	4.0–5.0	4.0–5.0	6.0–8.0	6.0–8.5	Rounded, conical or arrow	Phu Ho
NPA12	Dark blue–green	Straight, in mucus	3.0–5.5	5.0–6.0–10.0	4.0–6.0	5.0–8.0	7.0–10.0	8.0–14.0	Rounded conical or sometimes pointed conical	Phu An
APM3	Yellowish green	Straight and arranged in parallel	3.5–4.0	5.0–6.0	5.0–6.0	5.0–7.0	5.0–9.0	7.0–8.0	Rounded	Phu My
PA2	Blue–green	Straight	3.0–5.0	3–7–9	4.0–6.0	7.0–8.0	7.5–9.0	9.0–10	Rounded, conical or arrow	Phu An

Note: Samples were collected from the paddy soils of four communes, including Phu An, Phu Duong, Phu Ho, and Phu My in Phu Vang district, Thua Thien Hue province, Vietnam.

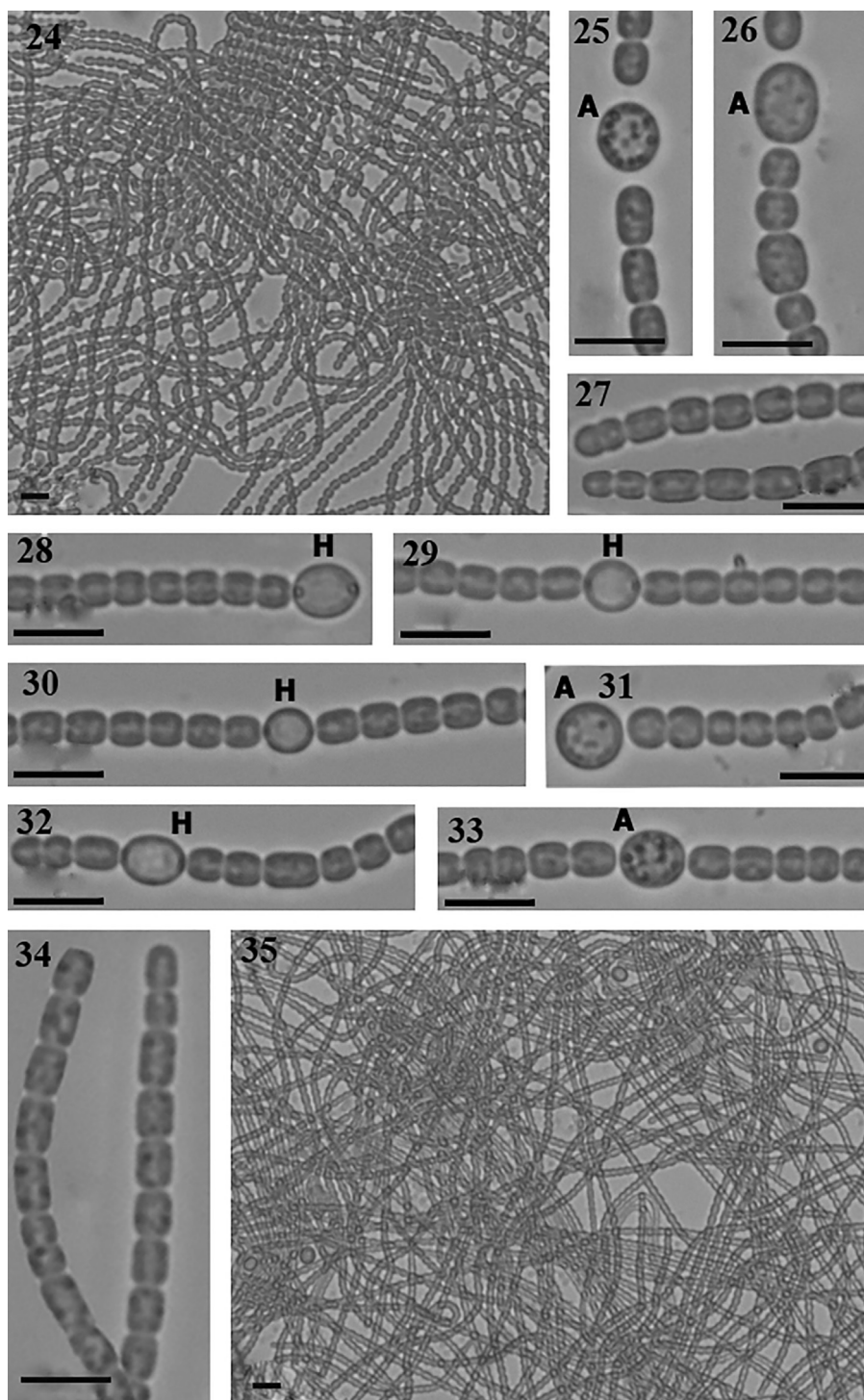


Fig. 3. 24–29. Strain APD3. 24 – Trichomes in a mass. 25, 26. Trichomes with akinetes (A). 27 – Straight trichomes. 28, 29 – Trichomes with heterocytes (H). 30–35. Strain APD4. 35 – Trichomes in a mass. 34 – Straight trichomes. 30, 32 – Trichomes with heterocytes. 31, 33 – Trichomes with akinetes. Scale bars = 10 μm .

MrBayes with phylogenetic support from both ML and BI analyses is shown in Fig. 6.

Sequence analysis revealed that eight strains (APA4, APA5, APA9, NPA1, NPA6, APD3, APD4, and APH5) shared 100% sequence similarity. Similarly, strains APH4 and NPA12 also had identical sequences. Three additional genotype groups were identified, each corresponding to single strain APM3, NMA2, or PA2 (Fig. 6). In total, 13 strains were divided into five genotypic groups based on 16S rRNA gene sequences with sequence similarities between these

groups ranging from 93.22% to 98.58%, and sequence similarities to the most closely related taxa in the public databases ranging from 98.14% to 99.78% (Fig. 7).

Bioactivities

Cytotoxic activity

All 26 crude extracts from 13 cyanobacterial strains were assessed for cytotoxicity against three human cancer cell lines

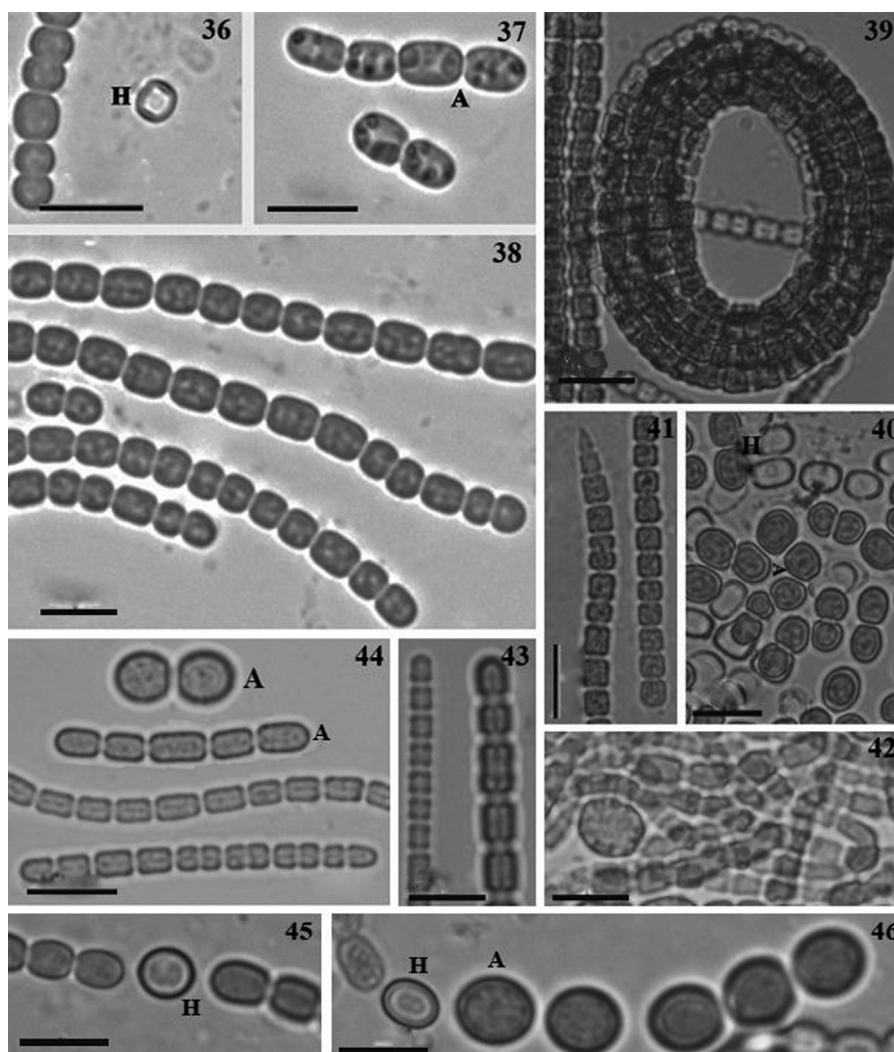


Fig. 4. 36–38. Strain APH5. 36 – Heterocyte. 37 – Akinetes. 38 – Straight trichomes. 39–41. Strain NMA2. 39 – Straight trichomes in a mass. 40 – Trichomes with akinetes (A) and heterocytes (H). 41 – Trichomes attenuated at the end or round end. 42–46. Strain PA2. 42 – Trichomes in a mass. 43 – Straight trichomes. 44 – 46. Trichomes with akinetes and heterocytes. Scale bars = 10 μm .

MCF7, HCT116 and HepG2 at five concentrations ranging from 25 to 400 $\mu\text{g mL}^{-1}$. The results indicated that three strains (APA4, APA5 and APD4) exhibited cytotoxic activities with IC_{50} values ranging from 47.8 $\mu\text{g mL}^{-1}$ to 232.0 $\mu\text{g mL}^{-1}$ (Fig. 8). The highest inhibitory activity against MCF7 and HCT116 cells was found using APD4-EtAc extract with IC_{50} values of 54.5 $\mu\text{g mL}^{-1}$ and 47.8 $\mu\text{g mL}^{-1}$, respectively. The methanol extract of the APD4 strain had lower cytotoxicity to MCF7 cancer cells, as well as HCT116, with IC_{50} values from 131.8 $\mu\text{g mL}^{-1}$ to 232.2 $\mu\text{g mL}^{-1}$. Similar to strain APA4, the ethyl acetate extract inhibited growth of HCT116 cells more strongly (IC_{50} 109.2 $\mu\text{g mL}^{-1}$) than the methanol extract (IC_{50} 168.9 $\mu\text{g mL}^{-1}$). However, only the methanol extract of strain APA5 revealed cytotoxic activity to MCF7 cells with an IC_{50} value of 112.1 $\mu\text{g mL}^{-1}$, since the ethyl acetate extract was not active. None of the 26 extracts prevented proliferation of HepG2 liver cancer cells, since treated cells grew well and showed normal shape even at the highest concentration of 400 $\mu\text{g mL}^{-1}$.

Antibacterial activity

Four bacteria species were used as targets for screening the antibacterial activities of 26 extracts prepared from the biomass of 13 cyanobacterial strains. The results showed that 14 extracts from

11 strains inhibited growth of the bacteria tested. Among these, two methanol extracts from strains APA5 and APD4 showed strong activity against both Gram-negative bacteria (*S. flexneri* and *S. typhi*) and Gram-positive bacteria (*S. aureus* and *B. subtilis*), with inhibition zones ranging from 12.8 to 23.3 mm in diameter (Table 2). Twelve methanol and ethyl acetate extracts derived from seven strains (APA4, APA9, APD3, AHP5, NPA1, NPA6 and NMA2) had weak to moderate activity to the tested bacteria with inhibition zones ranging from 9.7 to 12.7 mm. Overall, the activities were more potent towards Gram-positive than Gram-negative bacteria, and the methanol extracts displayed stronger activities than the ethyl acetate extracts. In addition, the methanol extracts from APH4 and NPA12 showed weak activity only to Gram-positive bacteria with inhibition zones below 8.3 mm. Neither methanol nor ethyl acetate extracts from the APM3 and PA2 strains exhibited any inhibitory activity towards the tested bacteria.

Discussion

The combination of morphological and molecular characterization confirmed the taxonomic placement of 13 cyanobacterial strains in the genus *Nostoc sensu lato*. These strains displayed a

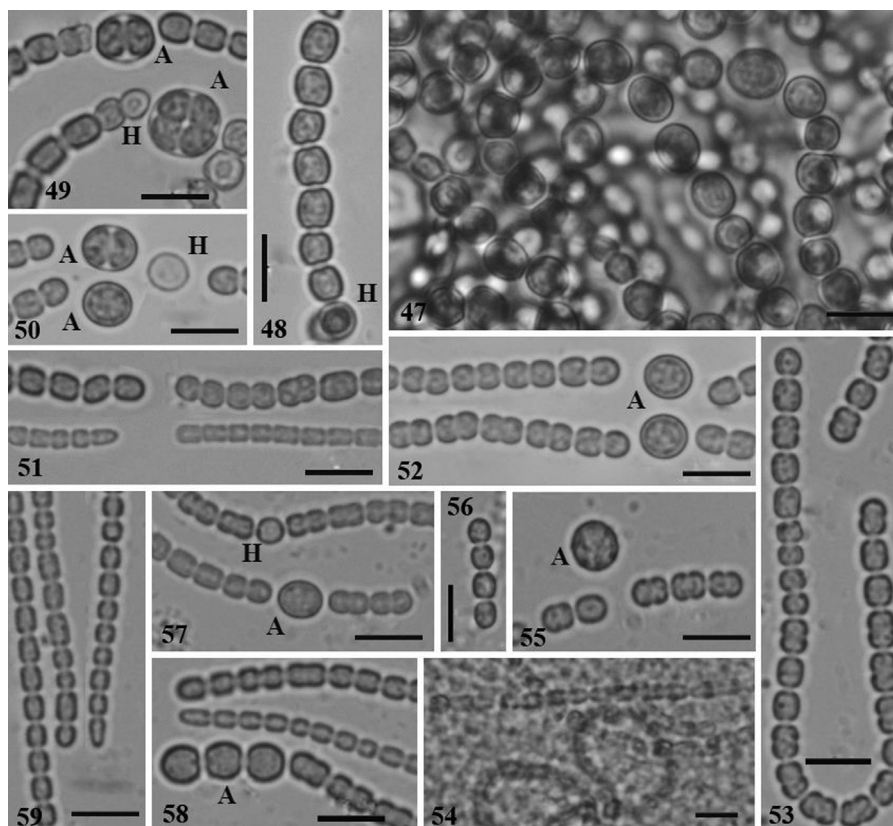


Fig. 5. 47–52. Strain NPA12. 47. Trichomes in a mass. 48–52 – Trichomes with akinetes (A) and heterocysts (H). 53–56. Strain APM3. 54 – Trichomes in mucus. 53, 56 – Straight trichomes. 55 – Trichome and akinete. 57–59. Strain APH4. 57 – Trichome with heterocysts. 58 – Trichomes with akinetes. 59 – Straight trichomes. Scale bars = 10 μm.

Table 2
Inhibition zones of 26 cyanobacterial extracts against Gram-positive and Gram-negative bacteria.

Group	Strains	Extracts	Inhibition zone (mm) ^a			
			<i>S. aureus</i>	<i>B. subtilis</i>	<i>S. flexneri</i>	<i>S. typhi</i>
Clade A	APA4	APA4-EtAc	0.0	0.0	0.0	0.0
		APA4-Met	12.7 ± 1.2	14 ± 1.0	11.3 ± 0.6	10 ± 1.0
	APA5	APA5-EtAc	9.5 ± 1.8	9.7 ± 0.6	9.5 ± 0.5	10.3 ± 0.8
		APA5-Met	16.3 ± 1.2	16.8 ± 0.8	13.5 ± 0.5	14 ± 1.0
	APA9	APA9- EtAc	6.5 ± 0.5	6.8 ± 0.8	9.7 ± 0.6	0.0
		APA9- Met	12.2 ± 0.3	12.7 ± 0.6	10.8 ± 0.3	9.7 ± 0.6
	APD3	APD3- EtAc	0.0	0.0	0.0	0.0
		APD3- Met	11.7 ± 0.6	11.0 ± 0.0	9.3 ± 0.6	10.0 ± 0.0
	APD4	APD4-EtAc	0.0	0.0	0.0	0.0
		APD4- Met	21.3 ± 1.5	23.3 ± 0.6	18.2 ± 0.8	12.8 ± 0.8
	APH5	APH5-EtAc	0.0	0.0	0.0	0.0
		APH5-Met	10.8 ± 0.3	11.7 ± 0.6	10.3 ± 0.6	11.8 ± 0.8
	NPA1	NPA1-EtAc	0.0	0.0	0.0	0.0
		NPA1-Met	9.7 ± 0.3	10.2 ± 0.6	9.8 ± 0.8	10.2 ± 1.3
	NPA6	NPA6-EtAc	0.0	0.0	0.0	0.0
		NPN6-Met	10.0 ± 1.0	11.7 ± 1.5	9.0 ± 1.0	9.3 ± 0.6
	APH4	APH4-EtAc	0.0	0.0	0.0	0.0
		APH4-Met	7.0 ± 0.5	7.2 ± 0.8	0.0	0.0
	NPA12	NPA12-EtAc	0.0	0.0	0.0	0.0
		NPA12-Met	8.3 ± 0.6	8.2 ± 1.0	0.0	0.0
APM3	APM3-EtAc	0.0	0.0	0.0	0.0	
	APM3-Met	0.0	0.0	0.0	0.0	
PA2	PA2-EtAc	0.0	0.0	0.0	0.0	
	PA2-Met	0.0	0.0	0.0	0.0	
Clade B	NMA2	NMA2-EtAc	9.9 ± 0.5	9.7 ± 0.8	0.0	0.0
		NMA2-Met	11.0 ± 0.5	11.3 ± 0.6	0.0	0.0

N.B. Strong activities: 15 mm ≤ inhibition zones < 25 mm; moderate activities: 10 mm ≤ inhibition zones < 15 mm; weak activities: 6 mm ≤ inhibition zones < 10 mm; no activity: < 6 mm; n = 3 with two replicates; 2 mg extract/6 mm paper disc.

^a Inhibition zone including diameter of paper disc.

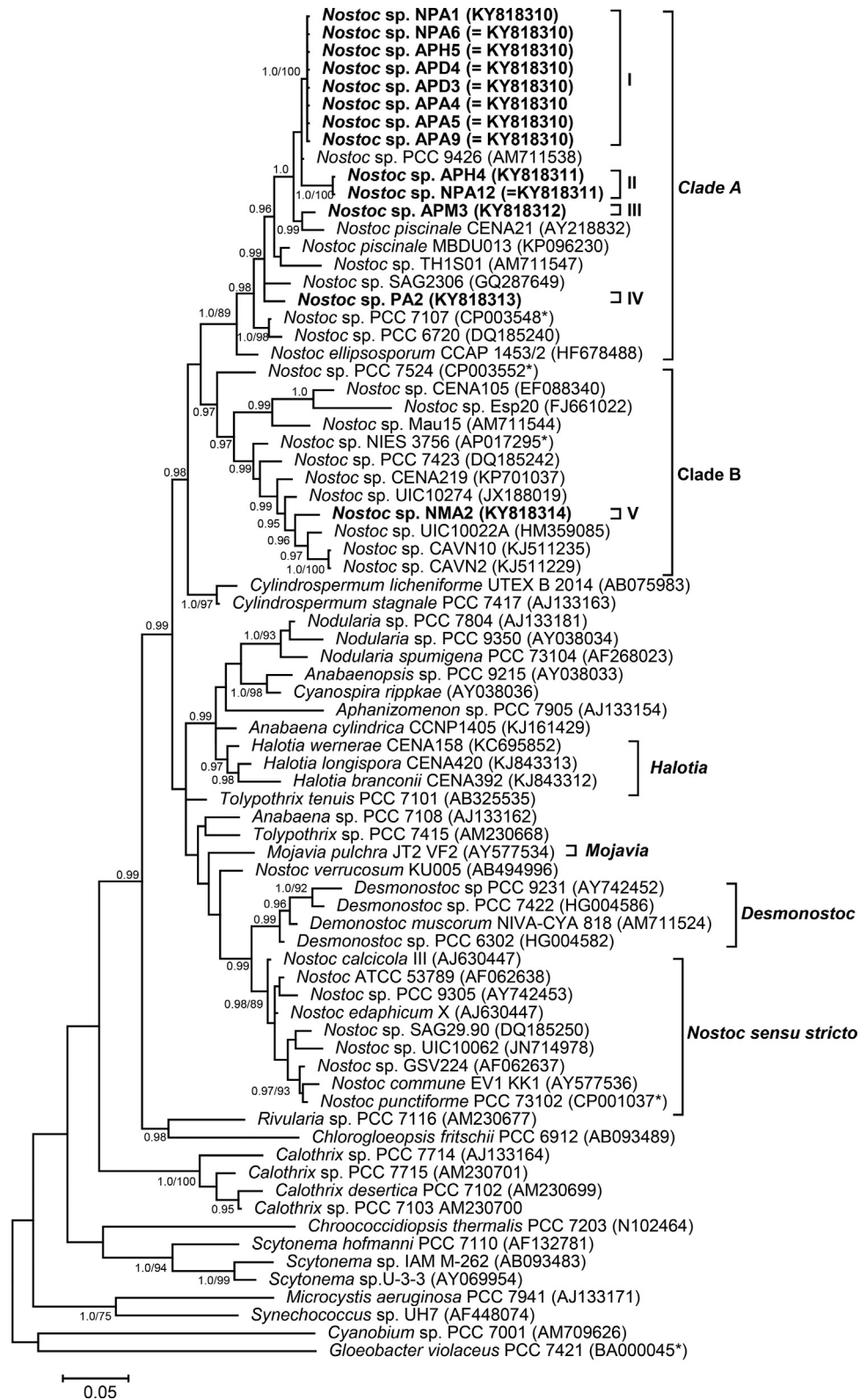


Fig. 6. Phylogram derived from Bayesian analyses of 16S rDNA sequence dataset. The analyses were conducted for 10 independent runs using MrBayes v3.2.5, each run was carried out for 5 million generations, applying the GRT + G + I substitution model. Bayesian posterior probabilities (BPP) greater than 95% and maximum likelihood (ML) values greater than 70 are indicated at the nodes as BPP or BPP/ML. Scale bar indicates estimated substitutions per site.

higher level of phenotypic diversity than genotypic diversity (based on 16S rRNA profiling), in which seven morphotypes were grouped into five genotypes. Given the limited sampling schemes used in the study, this suggests a high level of diversity for *Nostoc* species from

this geographic region. Five genotypes formed two distinct clades, which were well supported by phylogenetic analysis of 16S rRNA sequences. Four of the five identified genotypes were included in clade A and one genotype belonged to clade B (Fig. 6).

	1	2	3	4	5	6	7	8	9	10	11	12	13	14	15	16	17	18
<i>Nostoc</i> sp. APH4	1	13	15	20	24	29	23	34	32	32	54	62	59	62	47	56	54	52
<i>Nostoc</i> sp. PCC 9426	2	98.58		2	14	11	21	14	25	26	23	44	58	54	51	54	48	45
<i>Nostoc</i> sp. NPA1	3	98.36	99.78		16	13	19	16	23	28	25	44	57	53	50	53	46	43
<i>Nostoc piscinale</i> CENA21	4	97.81	98.47	98.25		14	29	22	27	20	27	52	61	57	55	58	40	45
<i>Nostoc</i> sp. APM3	5	97.37	98.80	98.58	98.47		31	21	29	26	19	52	60	55	54	62	42	39
<i>Nostoc ellipsosporum</i> CCAP 1453/2	6	96.82	97.70	97.92	96.82	96.60		21	19	30	28	35	49	40	40	42	49	47
<i>Nostoc piscinale</i> MBDU013	7	97.48	98.47	98.25	97.59	97.70	97.70		17	21	18	41	57	54	52	57	53	50
<i>Nostoc</i> sp. PCC 7017	8	96.28	97.26	97.48	97.05	96.83	97.92	98.14		21	18	41	59	50	48	57	51	48
<i>Nostoc</i> sp. SAG2306	9	96.50	97.16	96.94	97.81	97.16	96.72	97.70	97.70		15	46	61	48	51	57	49	54
<i>Nostoc</i> sp. PA2	10	96.50	97.48	97.26	97.05	97.92	96.94	98.03	98.36		41	57	45	49	59	49	42	46
<i>Nostoc</i> sp. PCC 7524	11	94.09	95.18	95.18	94.30	94.30	96.17	95.51	95.51	94.97	95.51		46	39	42	46	56	51
<i>Nostoc</i> sp. NMA2	12	93.22	93.65	93.76	93.33	93.44	94.64	93.77	93.54	93.33	93.76	94.97		21	22	23	57	51
<i>Nostoc</i> sp. PCC 7423	13	93.54	94.09	94.20	93.76	93.98	95.62	94.10	94.53	94.75	95.08	95.73	97.70		19	26	53	47
<i>Nostoc</i> sp. CENA219	14	93.22	94.42	94.53	93.98	94.09	95.62	94.32	94.75	94.42	94.64	95.40	97.59	97.92		25	55	52
<i>Nostoc</i> sp. CAVN10	15	94.85	94.09	94.19	93.65	93.21	95.40	93.76	93.76	93.76	93.54	94.96	97.48	97.16	97.26		65	63
<i>Nostoc punctiforme</i> PCC 73120	16	93.87	94.75	94.97	95.62	95.40	94.64	94.21	94.42	94.64	94.64	93.87	93.76	94.20	93.98	92.89		9
<i>Nostoc</i> sp. ATCC 53789	17	94.09	95.08	95.30	95.08	95.73	94.86	94.54	94.75	94.09	95.40	94.42	94.42	94.86	94.31	93.11	99.02	
<i>Nostoc</i> sp. PCC 9305	18	94.31	95.08	95.30	95.08	95.30	94.86	94.54	94.75	94.09	94.97	94.42	94.64	94.86	94.53	93.33	98.36	99.12

Fig. 7. Pair-wise comparisons of number of nucleotide differences (upper diagonal) and percentage identities (lower diagonal) of the 16S gene region between isolated strains described in this study and other related nostocacean isolates. The total alignment length was 915 bp including gap positions. For two groups of strains with identical sequences (NPA12 = APH4, and APA4 = APA5 = APA9 = APD3 = APD4 = APH5 = NPA1 = NPA6) only one representative strain per group was included.

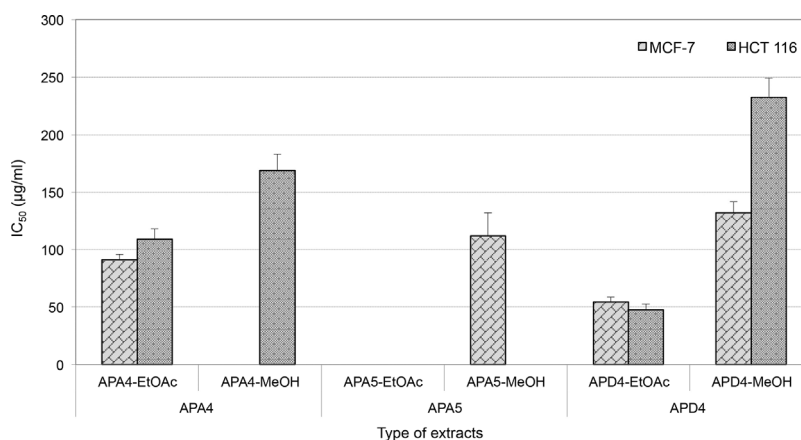


Fig. 8. IC₅₀ value of several positive extracts tested for inhibition of cancer cell lines. MCF-7 = human breast adenocarcinoma and HCT116 = colon carcinoma cells. Each type of extract was incubated with cells for 48 h using four replicates and n = 3; mean ± SD.

Genotype I (similarity to other genotypes in clade A of 98.36% – genotype II, 98.58% – genotype III, and 97.26% – genotype IV): strain APH5 and seven strains with variations in the morphological features of morphotype I were included. These strains shared 98.50% sequence similarity to *Nostoc* sp. PCC 9426, which was also isolated from paddy soil in Egypt [34].

Genotype II (similarity to other genotypes in clade A of 98.36% – genotype I, 97.37% – genotype III, and 96.5% – genotype IV): despite belonging to two different morphotypes, strains APH4 and NPA12 revealed identical 16S rRNA gene sequences, similar to the results found for the two morphospecies *Nostoc commune* VB516200 and *Nostoc punctiforme* VB51286, although they were classified into the same clades based on 16S rRNA gene sequences [24].

Genotype III (similarity to other genotypes in clade A of 98.58% – genotype I, 97.37% – genotype II, 97.92% – genotype IV): including strain APM3, which was grouped with strain *Nostoc piscinale* CENA21 isolated from sediment in the Brazilian Amazon floodplain [14].

Genotype IV (similarity to other genotypes in clade A of 97.26% – genotype I, 96.50% – genotype II, and 97.92% – genotype III): contained strain PA2, which was closely related to *Nostoc* sp. SAG 2306, isolated from a clay soil sample in Egypt [1].

Genotype V (clade B, similarity to other genotypes in clade A of 93.22% – 93.76%): consisted of only single strain NMA2. This strain was classified into a different clade that also included two strains, *Nostoc* sp. CAVN 10 and *Nostoc* sp. CAVN 2, isolated from Vietnam [6,36]. These strains were also isolated from soil samples in North-

ern Vietnam, which suggests their similar ecology. However, the 16S rRNA sequence similarity between these strains was 97.48%.

Although the morphological, molecular, and habitat data of the 13 strains used in this study supported the close relationship to *Nostoc* reference strains from previous studies, based on molecular phylogeny, not all strains belonged to *Nostoc sensu stricto* or any of the recently described new genera (*Desmonostoc*, *Mojavia*, and *Halotia*) [16,20,38] (Fig. 6). Instead, together with other available sequences, they formed two distinct lineages (clade A and clade B), which might represent separate genera. However, further clarification will need in-depth classification and consideration following the recommendation by Hrouzek et al. [20] before any conclusion concerning their generic identity is possible.

Together with molecular and morphological characterization, the biological activities of intracellular extracts from 13 strains were screened to determine any possible correlation between the taxonomic classification and biological activity, and to evaluate their pharmaceutical potential. The antibacterial activities were mostly found in extracts from strains belonging to genotypes I and V (represented by strains NPA1 and NMA2). Extracts from strains APM3 and PA2 did not show any inhibition activity towards test bacteria. Despite having identical 16S rRNA gene sequences, extracts of eight strains from genotype I displayed different antibacterial activities, and only three of them inhibited the growth of cancer cells. These differences in biological activities seemed to be caused by differences in the array of natural compounds produced by the strains, as described previously for *Nostoc*

spp. CAVN2 and CAVN10 [36]. Although strain NMA2 resided in the same clades with other cyclophane-producing cyanobacterial strains, such as *Nostoc* spp. CAVN2, CAVN10 and UIC10022A [10], the bioactivity of its biomass extract was noticeably weaker in comparison with the other strains. Primary analysis (unpublished data) had indicated that NMA2 did not produce any cyclophane-related compounds.

The genotype–chemotype relationship in cyanobacteria has been investigated in several studies [50,55], however, only low correlation has been found between 16S rRNA gene sequences and the chemical profile in several genera, such as *Lyngbya*, *Symphloca*, *Dolichospermum* and *Sphaerospermopsis*. For the first time, the present study showed variable bioactivity of *Nostoc* species strains even though they had similar 16S rRNA gene sequences. Most probably, the gene and/or pathways responsible for producing these metabolites are highly variable within certain species/clades, leading to the observed variability of the metabolic profiles [30]. Thus, the bioactivity of one strain cannot be assumed based on its 16S rRNA gene sequence or its relationship to other strains in a phylogenetic tree.

The pharmaceutical potential of cyanobacteria belonging to the *Nostoc* genus has been well documented. Although the natural compounds isolated from *Nostoc* strains have shown enzyme inhibitor activities or antiviral activities, they have mostly exhibited antibacterial and cytotoxic activities [8,12,45,48]. By testing fractions of crude extracts prepared from cyanobacterial biomass, Hrouzek et al. [19] concluded that the specific secondary metabolites appearing in the extract, rather than the primary metabolites or the whole extract itself, were responsible for cytotoxicity. To date, a series of strong antibacterial and cytotoxic substances, such as nostocycline A, insulapeptolide A, noscomin, borophycin, banyaside B, nostocarbolone, merocyclophane C–D, etc., have been discovered from the genus *Nostoc* [29,33]. Cryptophycins isolated from *Nostoc* sp. ATCC 53789 and subsequently from *Nostoc* sp. GSV 224 [17,47] have especially shown high cytotoxicity against multi-drug resistant cancer cells and were considered as potent payloads for antibody drug conjugates in cancer treatment [51,53]. From this current study, it is worth mentioning that extracts from strains APA4, APA5 and APD4 not only had cytotoxic activities but also exhibited stronger antibacterial activities than those from all the remaining strains. This result indicated that these strains could be potential sources for isolation of substances with pharmaceutical potential.

In conclusion, 13 cyanobacterial strains from soil samples were assigned to five genotypic groups representing seven morphotypic groups. There were good agreements between 16S rRNA gene characterization and morphological features. Strains with identical 16S rRNA gene sequences displayed different antibacterial as well as cytotoxic activities. Methanol extracts from strains APA4, APA5 and APD4 showed the most potent antibacterial activities. These were also the only strains that exhibited cytotoxic activities against breast adenocarcinoma cells and colon carcinoma cells.

Acknowledgements

This research was funded by the Vietnam National Foundation for Science and Technology Development (NAFOSTED) [grant number 106.16–2012.24]. We thank the Department of Pharmaceutical Biology, EMAU University, Greifswald, Germany for supporting a three-month research visit of the corresponding author of this study. We also thank Dr. Nguyen Thi Thuy Lien for useful discussion on morphological description, and Ms. Ngo Thi Trang for her excellent assistance in cultivation of cyanobacteria. We thank Prof. Ross Feldberg (Tufts University, USA) for proofreading the manuscript.

References

- [1] Abdel-Basset, R., Friedl, T., Mohr, K.I., Rybalka, N., Martin, W. (2011) High growth rate, photosynthesis rate and increased hydrogen(ases) in manganese deprived cells of a newly isolated *Nostoc*-like cyanobacterium (SAG 2306). *Int. J. Hydrogen Energy* 36, 12200–12210.
- [2] Andersen, R.A., Kawachi, M. (2005) Traditional microalgae isolation techniques. In: Andersen, R.A. (Ed.), *Algal Culturing Techniques*, Elsevier, Amsterdam, pp. 83–100.
- [3] Boyer, S.L., Flechtner, V.R., Johansen, J.R. (2001) Is the 16S–23S rRNA inter-nal transcribed spacer region a good tool for use in molecular systematics and population genetics? A case study in cyanobacteria. *Mol. Biol. Evol.* 18, 1057–1069.
- [4] Boyer, S.L., Johansen, J.R., Flechtner, V.R., Howard, G.L. (2002) Phylogeny and genetic variance in terrestrial *Microcoleus* (Cyanophyceae) species based on sequence analysis of the 16S rRNA gene and associated 16S–23S ITS region. *J. Phycol.* 38, 1222–1235.
- [5] Bravakos, P., Kotoulas, G., Skaraki, K., Pantazidou, A., Economou-Amilli, A. (2016) A polyphasic taxonomic approach in isolated strains of Cyanobacteria from thermal springs of Greece. *Mol. Phylogenet. Evol.* 98, 147–160.
- [6] Bui, H.T., Jansen, R., Pham, H.T., Mundt, S. (2007) Carbamidocyclophanes A–E, chlorinated paracyclophanes with cytotoxic and antibiotic activity from the Vietnamese cyanobacterium *Nostoc* sp. *J. Nat. Prod.* 70, 499–503.
- [7] Chakdar, H., Pabbi, S. (2017) A comparative study reveals the higher resolution of RAPD over ARDRA for analyzing diversity of *Nostoc* strains. *3 Biotech.* 7, 125.
- [8] Chlipala, G.E., Mo, S., Orjala, J. (2011) Chemodiversity in freshwater and terrestrial cyanobacteria – a source for drug discovery. *Curr. Drug Targets* 12, 1654–1673.
- [9] Chlipala, G.E., Pham, H.T., Nguyen, V.H., Krunic, A., Shim, S.H., Soejarto, D.D., Orjala, J. (2010) Nhatrangins A and B, aplysiatoxin-related metabolites from the marine cyanobacterium *Lyngbya majuscula* from Vietnam. *J. Nat. Prod.* 73, 784–787.
- [10] Chlipala, G.E., Sturdy, M., Krunic, A., Lantvit, D.D., Shen, Q., Porter, K., Swanson, S.M., Orjala, J. (2010) Cyliindrocyclophanes with proteasome inhibitory activity from the cyanobacterium *Nostoc* sp. *J. Nat. Prod.* 73, 1529–1537.
- [11] Desikachary, T.V. 1959 Cyanophyta, Indian Council of Agricultural Research, New Delhi, pp. 686.
- [12] Dixit, R.B., Suseela, M.R. (2013) Cyanobacteria: potential candidates for drug discovery. *Antonie Van Leeuwenhoek* 103, 947–961.
- [13] Felczykowska, A., Pawlik, A., Mazur-Marzec, H., Toruńska-Sitarz, A., Narajczyk, M., Richert, M., Węgrzyn, G., Herman-Antosiewicz, A. (2015) Selective inhibition of cancer cells' proliferation by compounds included in extracts from Baltic Sea cyanobacteria. *Toxicol.* 108, 1–10.
- [14] Fiore, M.d.F., Neilan, B.A., Copp, J.N., Rodrigues, J.L., Tsai, S.M., Lee, H., Trevors, J.T. (2005) Characterization of nitrogen-fixing cyanobacteria in the Brazilian Amazon floodplain. *Water Res.* 39, 5017–5026.
- [15] Geitler, L. 1932 Cyanophyceae Rabenhorst's Kryptogamenflora von Deutschland, Österreich und Schweiz, vol. 14, Akademische Verlagsgesellschaft, Leipzig, pp. 1196.
- [16] Genuário, D.B., Vaz, M.G., Hentschke, G.S., Sant'Anna, C.L., Fiore, M.F. (2015) *Halotia* gen. nov., a phylogenetically and physiologically coherent cyanobacterial genus isolated from marine coastal environments. *Int. J. Syst. Evol. Microbiol.* 65, 663–675.
- [17] Golakoti, T., Ogino, J., Heltzel, C.E., Husebo, T.L., Jensen, C.M., Larsen, L.K., Patterson, G.M.L., Moore, R.E., Mooberry, S.L., Corbett, T.H., Valerios, F.A. (1995) Structure determination, conformational analysis, chemical stability studies, and antitumor evaluation of the Cryptophycins. Isolation of 18 new analogs from *Nostoc* sp. strain GSV-224. *J. Am. Chem. Soc.* 117, 12030–12049.
- [18] Hoffmann, L., Komárek, J., Kaštovský, J. (2005) System of cyanoprokaryotes (cyanobacteria) – state in 2004. *Algol. Stud.* 117, 95–115.
- [19] Hrouzek, P., Kapuščík, A., Vacek, J., Voráčová, K., Paichlová, J., Kosina, P., Voloshko, L., Ventura, S., Kopecký, J. (2016) Cytotoxicity evaluation of large cyanobacterial strain set using selected human and murine in vitro cell models. *Ecotoxicol. Environ. Saf.* 124, 177–185.
- [20] Hrouzek, P., Lukešová, A., Mareš, J., Ventura, S. (2013) Description of the cyanobacterial genus *Desmonostoc* gen. nov. including *D. muscorum* comb. nov. as a distinct, phylogenetically coherent taxon related to the genus *Nostoc*. *Fottea* 13, 201–213.
- [21] Hrouzek, P., Tomek, P., Lukešová, A., Urban, J., Voloshko, L., Pushparaj, B., Ventura, S., Lukavský, J., Štys, D., Kopecký, J. (2011) Cytotoxicity and secondary metabolites production in terrestrial *Nostoc* strains, originating from different climatic/geographic regions and habitats: is their cytotoxicity environmentally dependent? *Environ. Toxicol.* 26, 345–358.
- [22] Hrouzek, P., Ventura, S., Lukešová, A., Mugnai, M.A., Turicchia, S., Komárek, J. (2005) Diversity of soil *Nostoc* strains: phylogenetic and phenotypic variability. *Algol. Stud.* 117, 251–264.
- [23] Katoh, K., Standley, D.M. (2013) MAFFT multiple sequence alignment software version 7: improvements in performance and usability. *Mol. Biol. Evol.* 30, 772–780.
- [24] Keshari, N., Das, S.K., Adhikary, S.P. (2015) Identification of cyanobacterial species with overlapping morphological features by 16S rRNA gene sequencing. *Eur. J. Phycol.* 50, 395–399.
- [25] Komárek, J. (2016) A polyphasic approach for the taxonomy of cyanobacteria: principles and applications. *Eur. J. Phycol.* 51, 346–353.

- [26] Komárek, J., Anagnostidis, K. (1989) Modern approach to the classification system of Cyanophytes. 4 – Nostocales. *Algol. Stud.* 56, 247–345.
- [27] Komárek, J., Kaštovský, J., Mareš, J., Johansen, J.R. (2014) Taxonomic classification of cyanoprokaryotes (cyanobacterial genera) 2014, using a polyphasic approach. *Preslia* 86, 295–335.
- [28] Mateo, P., Perona, E., Berrendero, E., Leganés, F., Martín, M., Golubić, S. (2011) Life cycle as a stable trait in the evaluation of diversity of *Nostoc* from biofilms in rivers. *FEMS Microbiol. Ecol.* 76, 185–198.
- [29] May, D.S., Chen, W.L., Lantvit, D.D., Zhang, X., Kronic, A., Burdette, J.E., Eustaquio, A., Orjala, J. (2017) Merocyclophanes C and D from the cultured freshwater cyanobacterium *Nostoc* sp. (UIC 10110). *J. Nat. Prod.* 80, 1073–1080.
- [30] Mazur-Marzec, H., Bertos-Fortis, M., Torunska-Sitarz, A., Fidor, A., Legrand, C. (2016) Chemical and genetic diversity of *Nodularia spumigena* from the Baltic Sea. *Mar. Drugs* 14, 209.
- [31] Mishra, A.K., Shukla, E., Singh, S.S. (2013) Phylogenetic comparison among the heterocystous cyanobacteria based on a polyphasic approach. *Protoplasma* 250, 77–94.
- [32] Niedermeyer, T.H. (2015) Anti-infective natural products from Cyanobacteria. *Planta Med.* 81, 1309–1325.
- [33] Niedermeyer, T.H.J. (2014) Biologisch aktive Naturstoffe aus Cyanobakterien der Gattung *Nostoc*. *BIOSpektrum* 20, 151–153.
- [34] Papaefthimiou, D., Hrouzek, P., Mugnai, M.A., Lukesova, A., Turicchia, S., Rasmussen, U., Ventura, S. (2008) Differential patterns of evolution and distribution of the symbiotic behaviour in nostocacean cyanobacteria. *Int. J. Syst. Evol. Microbiol.* 58, 553–564.
- [35] Posada, D. (2008) jModelTest: phylogenetic model averaging. *Mol. Biol. Evol.* 25, 1253–1256.
- [36] Preisitsch, M., Harmrolfs, K., Pham, H.T., Heiden, S.E., Fussel, A., Wiesner, C., Pretsch, A., Swiatecka-Hagenbruch, M., Niedermeyer, T.H., Muller, R., Mundt, S. (2015) Anti-MRSA-acting carbamidocyclophanes H–L from the Vietnamese cyanobacterium *Nostoc* sp. CAVN2. *J. Antibiot. (Tokyo)* 68, 600.
- [37] Rajaniemi, P., Hrouzek, P., Kastovska, K., Willame, R., Rantala, A., Hoffmann, L., Komarek, J., Sivonen, K. (2005) Phylogenetic and morphological evaluation of the genera *Anabaena*, *Aphanizomenon*, *Trichormus* and *Nostoc* (Nostocales, Cyanobacteria). *Int. J. Syst. Evol. Microbiol.* 55, 11–26.
- [38] Řeháková, K., Johansen, J.R., Casamatta, D.A., Xuesong, L., Vincent, J. (2007) Morphological and molecular characterization of selected desert soil cyanobacteria: three species new to science including *Mojavia pulchra* gen. et sp. nov. *Phycologia* 46, 481–502.
- [39] Rippka, R., Duruelles, R., Waterbury, J.B., Herberman, M., Stanier, R.Y. (1979) Generic assignments, strain histories and properties of pure cultures of Cyanobacteria. *J. Gen. Microbiol.* 111, 1–61.
- [40] Ronquist, F., Teslenko, M., van der Mark, P., Ayres, D.L., Darling, A., Höhna, S., Larget, B., Liu, L., Suchard, M.A., Huelsenbeck, J.P. (2012) MrBayes 3.2: efficient Bayesian phylogenetic inference and model choice across a large model space. *Syst. Biol.* 61, 539–542.
- [41] Sciuto, K., Moro, I. (2015) Cyanobacteria: the bright and dark sides of a charming group. *Biodivers. Conserv.* 24, 711–738.
- [42] Sielaff, H., Christiansen, G., Schwecke, T. (2006) Natural products from cyanobacteria: exploiting a new source for drug discovery. *IDrugs* 9, 119–127.
- [43] Silva, C.S., Genuario, D.B., Vaz, M.G., Fiore, M.F. (2014) Phylogeny of culturable cyanobacteria from Brazilian mangroves. *Syst. Appl. Microbiol.* 37, 100–112.
- [44] Singh, R., Parihar, P., Singh, M., Bajguz, A., Kumar, J., Singh, S., Singh, V.P., Prasad, S.M. (2017) Uncovering potential applications of Cyanobacteria and algal metabolites in biology, agriculture and medicine: current status and future prospects. *Front. Microbiol.* 8, 515.
- [45] Singh, R.K., Tiwari, S.P., Rai, A.K., Mohapatra, T.M. (2011) Cyanobacteria: an emerging source for drug discovery. *J. Antibiot. (Tokyo)* 64, 401–412.
- [46] Stamatakis, A. (2014) RAxML version 8: a tool for phylogenetic analysis and post-analysis of large phylogenies. *Bioinformatics* 30, 1312–1313.
- [47] Subbaraju, G.V., Golakoti, T., Patterson, G.M., Moore, R.E. (1997) Three new cryptophycins from *Nostoc* sp. GSV 224. *J. Nat. Prod.* 60, 302–305.
- [48] Swain, S.S., Paidasetty, S.K., Padhy, R.N. (2017) Antibacterial, antifungal and antimycobacterial compounds from cyanobacteria. *Biomed. Pharmacother.* 90, 760–776.
- [49] Tan, L.T. (2007) Bioactive natural products from marine cyanobacteria for drug discovery. *Phytochemistry* 68, 954–979.
- [50] Thacker, R.W., Paul, V.J. (2004) Morphological, chemical, and genetic diversity of tropical marine cyanobacteria *Lyngbya* spp. and *Symploca* spp. (Oscillatoriales). *Appl. Environ. Microbiol.* 70, 3305–3312.
- [51] Verma, V.A., Pillow, T.H., DePalatis, L., Li, G., Phillips, G.L., Polson, A.G., Raab, H.E., Spencer, S., Zheng, B. (2015) The cryptophycins as potent payloads for antibody drug conjugates. *Bioorg. Med. Chem. Lett.* 25, 864–868.
- [52] Voigt, W. (2005) Sulforhodamine B assay and chemosensitivity. *Methods Mol. Med.* 110, 39–48.
- [53] Weiss, C., Figueras, E., Borbely, A.N., Sewald, N. (2017) Cryptophycins: cytotoxic cyclodepsipeptides with potential for tumor targeting. *J. Pept. Sci.* 23, 514–531.
- [54] Willame, R., Boutte, C., Grubisic, S., Wilmotte, A., Komárek, J., Hoffmann, L. (2006) Morphological and molecular characterization of planktonic cyanobacteria from Belgium and Luxembourg. *J. Phycol.* 42, 1312–1332.
- [55] Zapomelova, E., Hrouzek, P., Rezanka, T., Jezberova, J., Rehakova, K., Hisem, D., Komarkova, J. (2011) Polyphasic characterization of *Dolichospermum* sp. and *Sphaerospermopsis* spp. (Nostocales, Cyanobacteria): morphology, 16S rRNA gene sequences and fatty acid and secondary metabolite profiles. *J. Phycol.* 47, 1152–1163.